Supplementary Information

For

Environmental fluctuations accelerate molecular evolution of thermal tolerance in a marine diatom

C.-Elisa Schaum, A. Buckling, N. Smirnoff, D. Studholme & G. Yvon-Durocher

Correspondence to: c.l.schaum@exeter.ac.uk or g.yvon-durocher@exeter.ac.uk

This PDF file includes:

Figures:
Fig S1:Experimental Design
Fig S2: Trajectories of population size over the experimental period
Fig S3: Carbon-use efficiency in the lineages evolved under fluctuating warming.
Fig S4: Changes in macromolecular composition and cell size over acclimation and adaptation.
Fig S5: Light response curves for the photochemical efficiency of photosystem II.
Fig S6: Neighbour joining tree SNPS
Fig S7: Neighbour joining tree Phenotypic data

Tables:
Table S1: Summary of traits in ancestral and evolved populations.
Table S2. Model selection on generalized additive mixed effects model (GAMM) fitted to the trajectories of population growth.
Table S3. Model selection on generalized additive mixed effects model (GAMM) fitted to the trajectories of population size.
Table S4. Thermal tolerance curve parameters for the ancestor.
Table S5. Model selection and parameters of thermal tolerance curves of the evolved lineages.

Table S6: Model selection and parameters for the thermal responses of gross photosynthesis and respiration in the ancestor.
Table S7: Model selection and parameters for the thermal response of gross photosynthesis in the evolved lineages.
Table S8: Model selection and parameters for the thermal response of respiration in the evolved lineages.
Table S9: Model selection to determine the effects of selection regime on the carbon use efficiency.
Table S10: Model selection for the light response curves of photochemical efficiency (FRRF data).
Table S11: Model selection for C, N and P content, C:N, C:P, N:P, PPUE, PNUE, Chl:C ratio, size and silicate content, as well as ΦPSII at irradiance as in the incubator.
Table S12: PERMANOVA and pairwise comparison for differences between treatments (SNPs)
Table S13: PERMANOVA and pairwise comparison for differences between treatments (Phenotypes)
Table S14: Annotations for genes associated to specific treatments
Table S15: Aligned sequence depths for each sequenced population

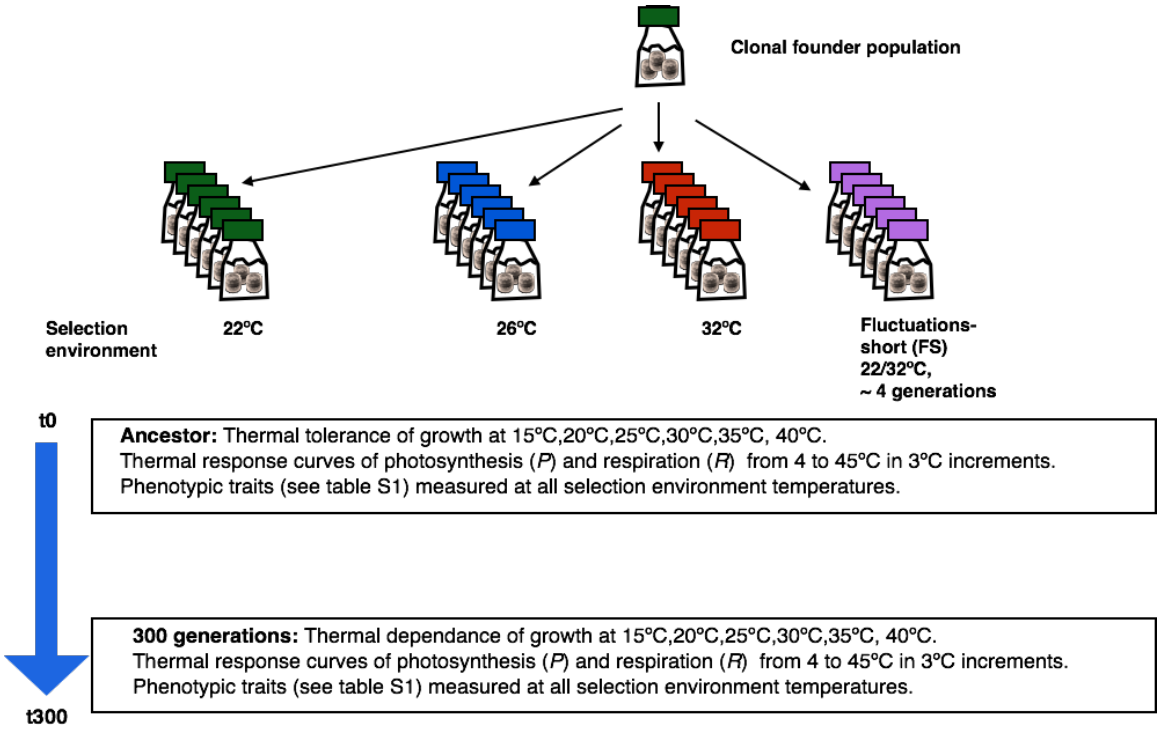

Figure S1 | Experimental design. Six biological replicates in four selection regimes (the control environment at 22ºC, a moderate warming environment at 26ºC, a severe environment at 32ºC, and an environment that cycled between 22ºC and 32ºC approximately every 4 generations "fluctuating – short" or "FS") were founded from a single clone, and then propagated through semi-continuous batch culture for at least 300 generations. The temperatures for moderate and extreme warming were chosen based on pilot data, which showed that 32ºC was past the optimum temperture for growth, but did not induce excessive mortality, and that 26ºC represented the predicted average increase in sea surface temperature according to the IPCC RCP4.5 scenario (+ 4ºC from ambient). The fluctuating environment represents a conceptually more likely scenario where organisms' experience only short periods of severe conditions followed by recovery of the benign environment. At the beginning of the experiment (t0), and at the end (t300), a wide range of metabolic and macromolecular traits were quantified in the ancestor and the evolved lineages (see methods).

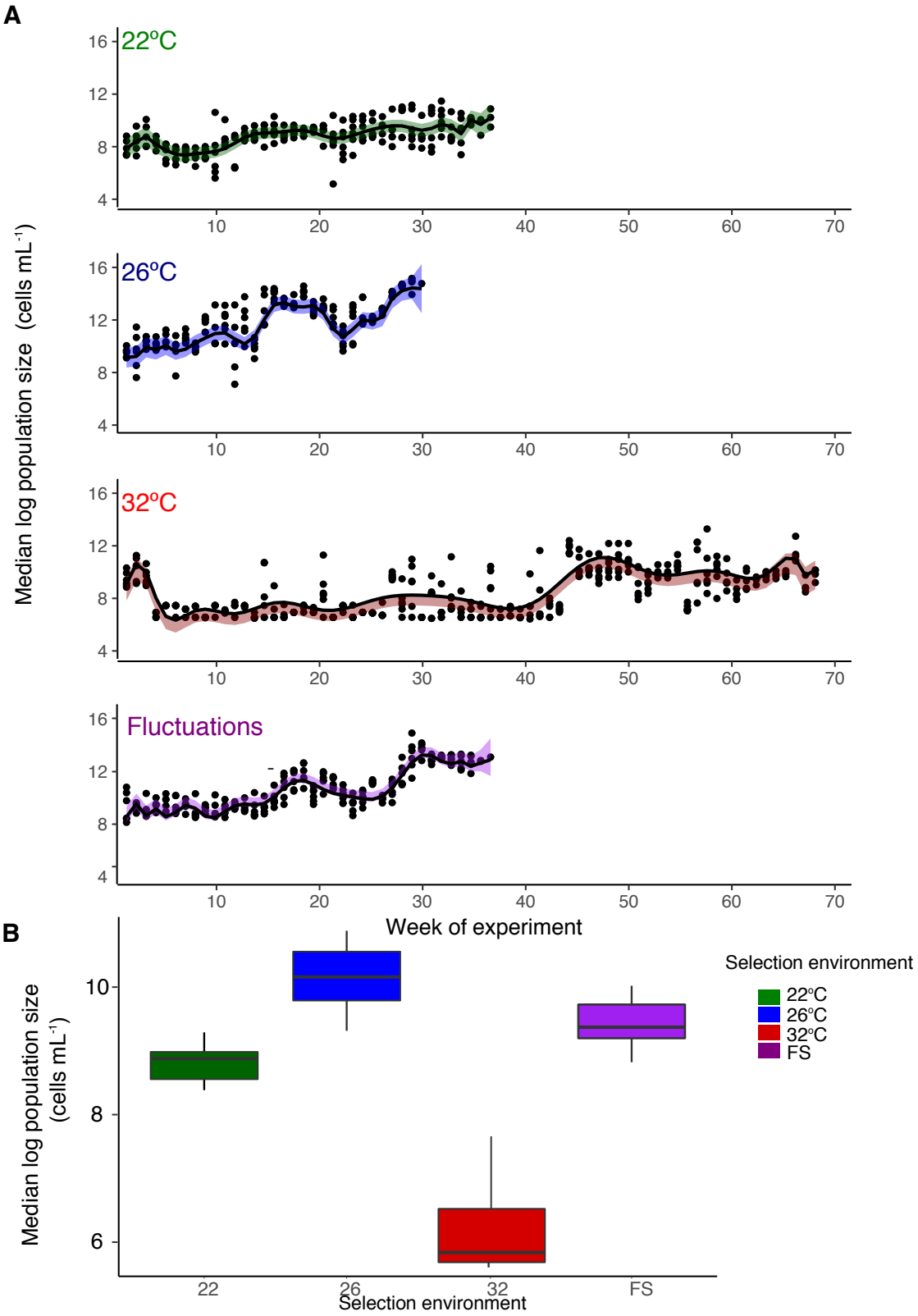
A
22ºC
26ºC
32ºC
Fluctuations
Median log population size (cells mL-1)
Week of experiment
B
Median log population size (cells mL-1)
Selection environment
22
26
32
FS
Selection environment
22ºC
26ºC
32ºC
FS

Figure | S2 Trajectories of population size over the selection experiment. (A) Trajectories of population size up to 300 generations determined from the cell density at the end of each transfer. Under moderate warming and in the fluctuating environment, there are rapid, sustained increases in population size. Under severe warming (32ºC), population size remained low until evolutionary rescue occurred after approximately 1 year (~ 100 generation). Although all samples received the same size inoculum at each transfer, mutational supply would have been larger in samples that attained higher population densities at the middle of the logarithmic phase of growth. Fitted lines are from the best fits of a GAMM (Table S3). (B) Boxplots of replicate level estimates (fixed and random effects of GAMM) for median population size for each environment calculated over 300 generations Median population size was highest in samples evolving under moderate warming and in the fluctuating environment, while those at 32ºC had the lowest average population size. Green samples are the control at 22ºC, blue is 26ºC, red is 32ºC, and purple is the fluctuating environment.

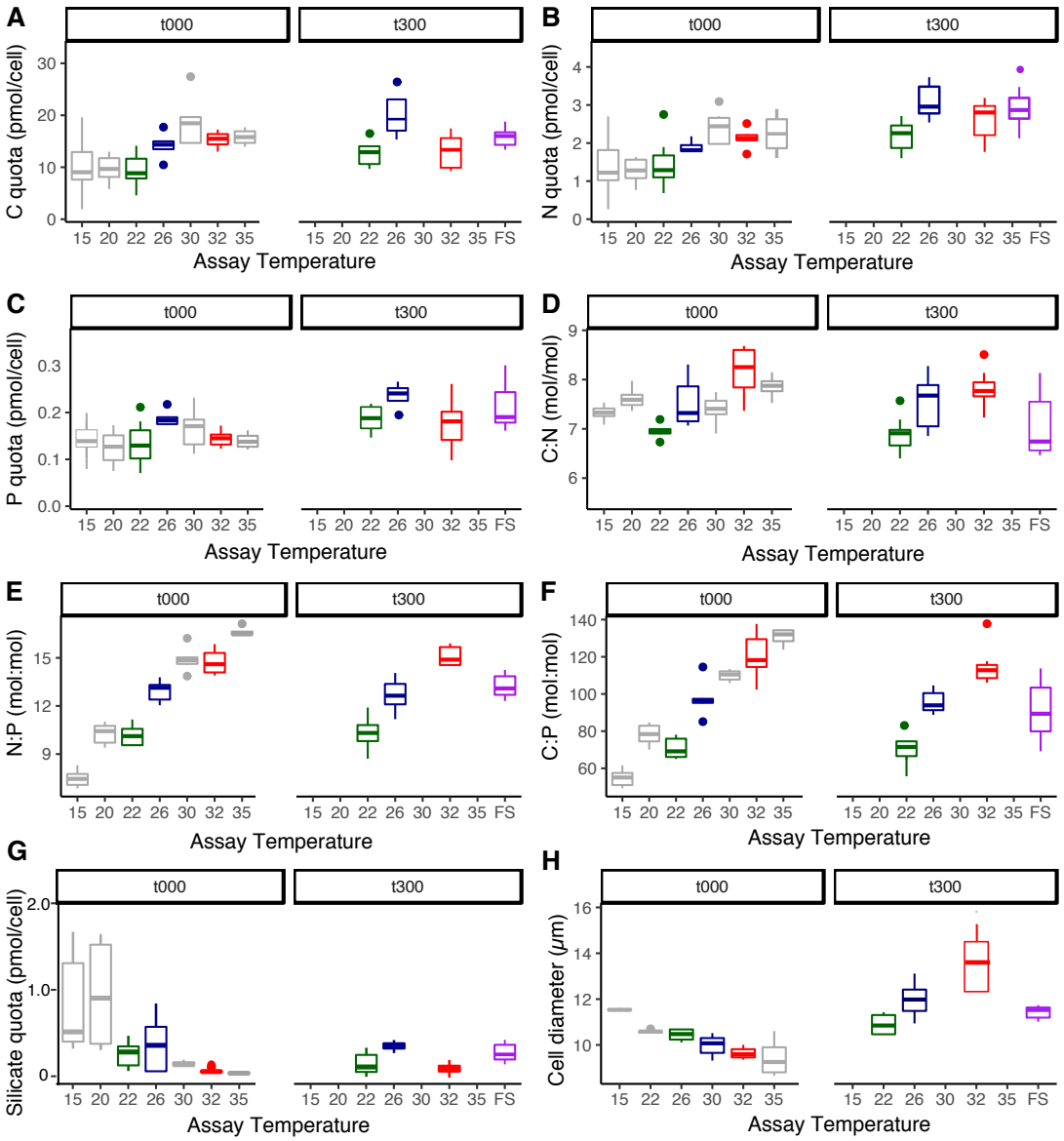

Figure S3 | Changes in macromolecular composition and cell size over acclimation and adaptation. Short-term thermal acclimation was investigated by exposing the ancestor at t000 to a 15 to 45ºC thermal gradient. The effects of long-term evolutionary adaptation to was quantified after 300 generations in the selection regimes. For elemental composition (C, N, P) and the resulting stoichiometry (C:N, C:P, N:P), the direction of acclimation was the same as that of the evolutionary response (panels A –F). G: Intracellular silicate content decreased with temperature in the short term, but samples at 26ºC and FS reestablished silicate contents similar to those of the ancestor and the control after 300 generations. H: Cell size decreased with temperature in the short term, but increased in the long-term, with the largest cells at 32ºC, and samples from the FS environment indistinguishable from samples from the 26ºC environment. For all boxplots, n=6. Grey denotes ancestor assay temperatures that were not used as selection

regimes. Green for selection and/or assay at 22ºC, blue at 26ºC, red at 32ºC and purple for the fluctuating environment (FS).

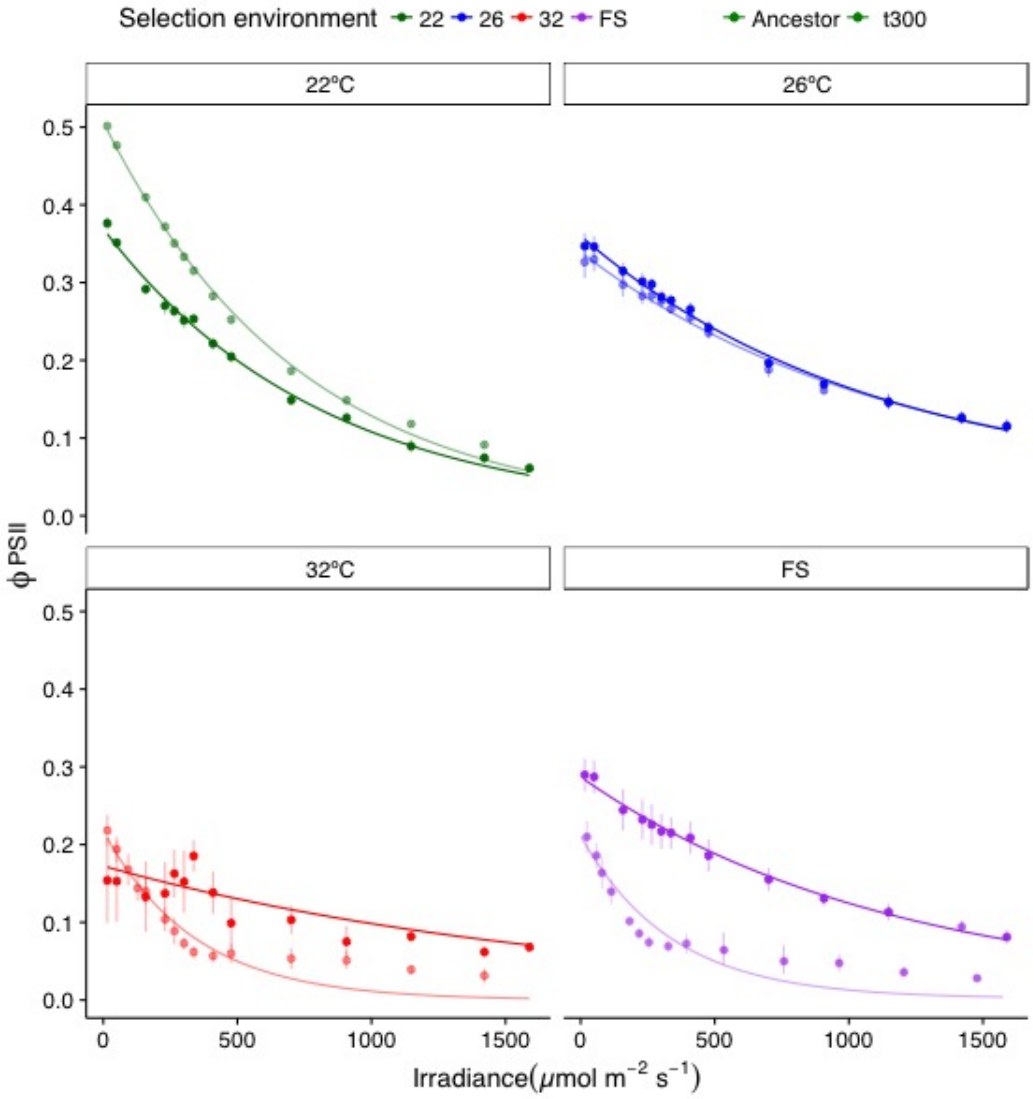

Figure S4| Light response curves for the photochemical efficiency of photosystem II. The light response curves for photochemical efficiency, ΦPSII, differed both among selection environments and between the evolved lineages and the ancestor. ΦPSII was the highest and declined less steeply with increasing irradiance in the moderate (26ºC) and fluctuating warming treatments. Lineages in the severe warming treatment (32ºC) had very low photochemical efficiency. Green denotes populations evolved at 22ºC, blue for samples evolved at 26ºC, red for 32ºC, and purple for the fluctuating environment, FS. The ancestor (faded colour) at each temperature is displayed alongside the evolved lineages. All values are means ± 1s.e.m. The fitted curves are derived from the best fits of a non-linear mixed effects model on Eq. (8).

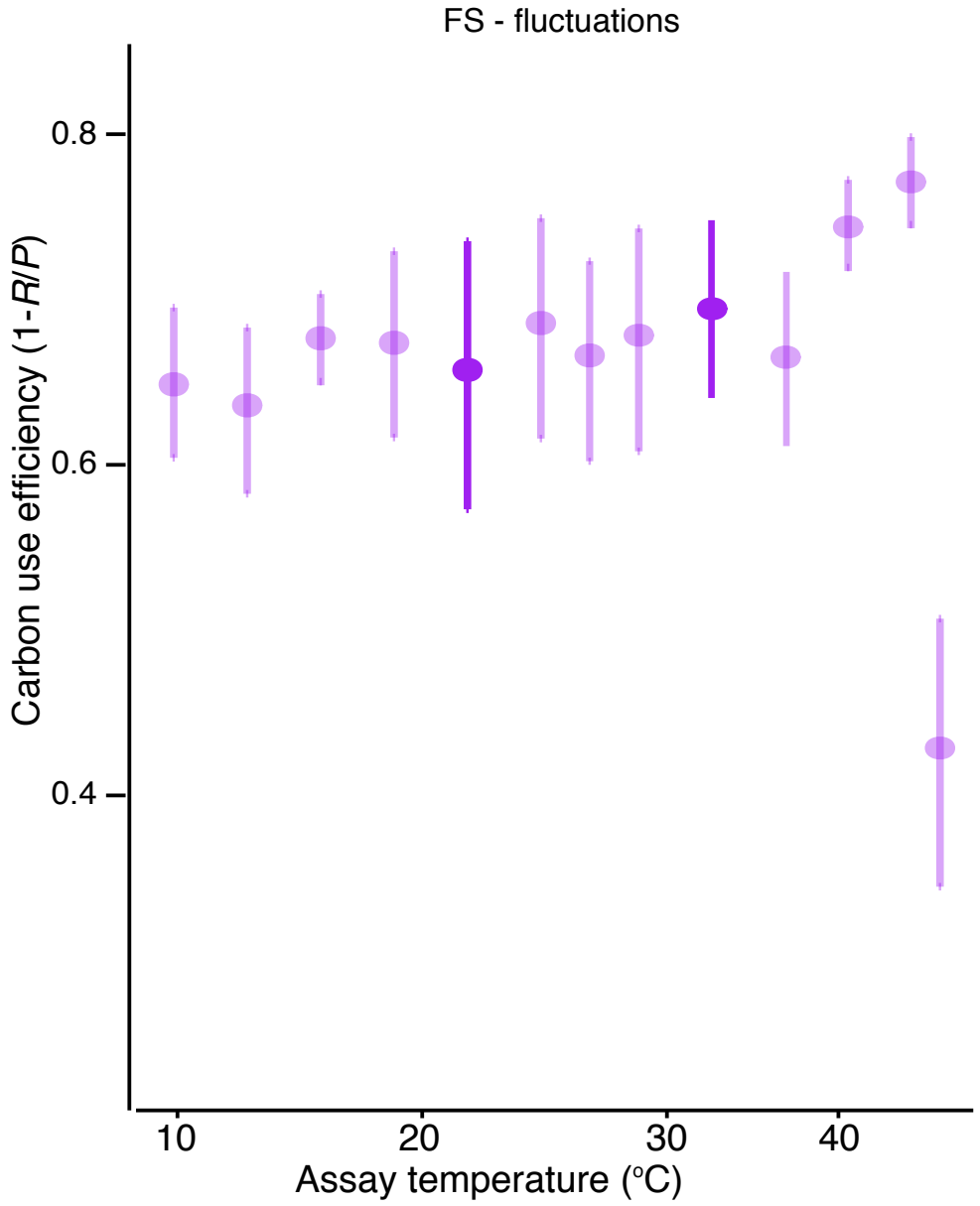

Figure S5| Carbon-use efficiency in the lineages evolved under fluctuating warming. Carbon-use efficiency (CUE) in the lineages evolved in the fluctuating environment (between 22 and 32ºC) did not differ significantly between assay temperatures spanning 10ºC to 35ºC. In the main manuscript, we present CUE at 32ºC for ease of comparison with the stable 32ºC selection environment. 22ºC and 32ºC are in bold, all other assay temperatures are faded. Data are displayed as means ± 1 s.e.m.

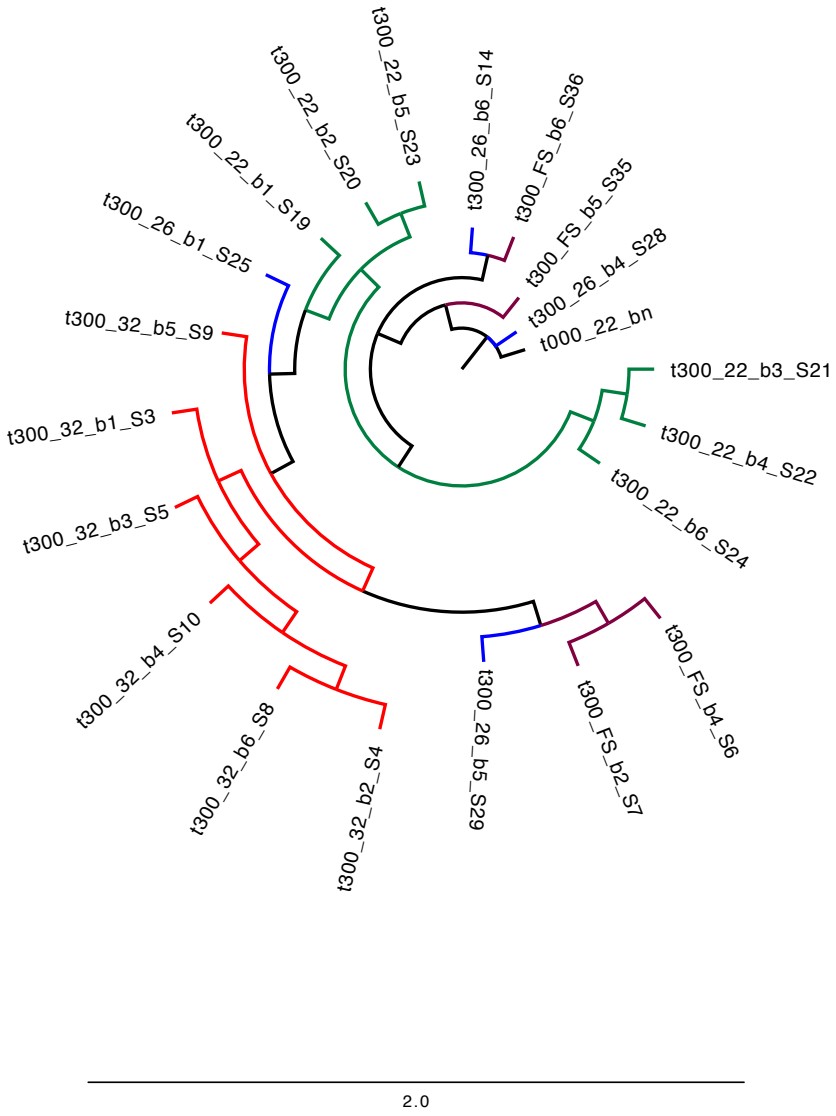

Figure S6| Neighbour joining tree based on Euclidean distances from frequency and identity of non-synonymous SNPs. The tree shows clustering of samples evolved at 22ºC and 32ºC with samples from the 26ºC and fluctuating selection regime intertwined with each other. Evolved samples are colour coded based on selection regime with green denoting control (22ºC), blue, moderate warming (26ºC), red, severe warming (32ºC), and purple, evolution in the fluctuating environment. The bar is indicative of the Euclidean distance.

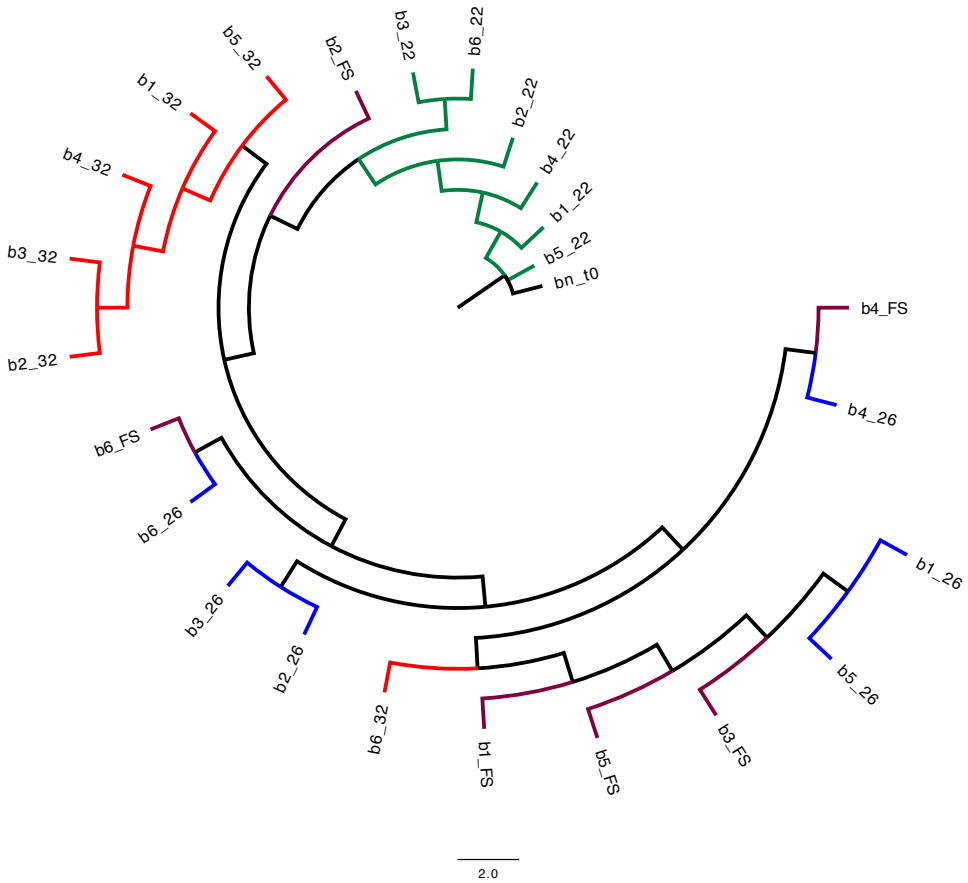

Figure S7| Neighbour joining tree based on Euclidean distances calculated from phenotypic trait values in the ancestor and evolved samples. Samples evolved at 22ºC cluster with each other and are most similar to the ancestor, whereas samples from the 26ºC and fluctuating selection regime intertwined with each other and show a greater distance to the ancestor. Evolved samples are colour coded based on selection regime with green denoting control (22ºC), blue, moderate warming (26ºC), red, severe warming (32ºC), and purple, evolution in the fluctuating environment. The bar is indicative of the Euclidean distance.

Table S1| Summary of traits in ancestral and evolved populations. All trait values were measured in the ancestor at 22ºC. After 300 generations, they were measured in the evolved samples at the temperature of their selection environment. Responses for samples evolved in the fluctuating treatment were measured at 22ºC, 26ºC 32ºC. For acute responses of FS-evolved lineages (i.e. metabolic traits and their thermal responses), they are displayed for 32ºC to aid comparison with the populations experiencing constant severe warming. All data are reported as means ± 1 s.e.m. Abbreviations and acronyms are used as follows: C for carbon, N for nitrogen, P for phosphate, M, for the assimilation quotient of CO_2:O_2**,** PPUE for phosphate use efficiency (growth per pg phosphate), PNUE for nitrogen use (growth per pg nitrogen), *P* as gross photosynthesis (µgC µgC $^{-1}$d^{-1}), *R* as respiration (µgC µgC $^{-1}$ d^{-1}), NP as net photosynthesis (µgC µgC $^{-1}$ d^{-1}), Φ_{PSII} as photosynthetic efficiency of PS II at 100µmol quanta m^{-2} s^{-1} (approximate light intensity in incubators), CUE as carbon use efficiency (1-*R*/*P*) and the metabolic traits describing the shape of unimodal thermal reaction norms are E_a, $P(T_c)$, $R(T_c)$, T_h, E_h and T_{opt}.

		Ancestor (at 22ºC)	22ºC	26ºC	32ºC	FS
Growth rate at t0 or t300		0.63± 0.13	0.77 ± 0.06	1.36 ± 0.05	0.63 ± 0.05	1.1 ± 0.08
Geometric mean growth rate		0.63± 0.13	0.71 ± 0.08	1.08 ±0 .11	0.24 ± 0.11	0.87 ± 0.12
Cellular traits	**Chl:C** (mg:mg)	0.024 ±0.007	0.071 ± 0.002	0.121 ± 0.002	0.088 ± 0.007	0.085 ± 0.007
	C:N (mol:mol)	7.07 ± 0.07	6.94 ± 0.12	7.08 ± 0.08	7.21 ± 0.14	7.18 ± 0.21
	C:P (mol:mol)	70.78 ± 2.87	69.91 ± 2.75	84.91 ± 2.21	112.93 ± 3.71	93.22 ± 8.99
	N:P (mol:mol)	10.16 ± 0.33	10.14 ± 0.39	12.75 ± 0.41	15.07 ± 0.26	13.21 ± 0.55
	M (CN/CN+2)	0.779	0.778	0.780	0.783	0.782
	C (pmol/cell)	9.97± 1.09	13.87 ± 0.81	19.66 ± 0.82	18.37 ± 1.12	19.21 ± 0.75
	N (pmol/cell)	1.41 ± 0.14	1.98 ± 0.09	2.76 ± 0.13	2.53 ± 0.08	2.67±0.11
	P (pmol/cell)	0.139 ± 0.017	0.13± 0.009	0.216 ± 0.008	0.168 ± 0.019	0.202 ± 0.016
	Silicate (pmol /cell)	0.353 ± 0.061	0.317 ± 0.025	0.346 ± 0.023	0.168 ± 0.077	0.311 ± 0.02
	Volume (µm^3)	3794.25 ± 680.96	3610.65 ± 789.14	6359.75 ±818.17	13582.53 ± 692.95	4643.54 ± 673.61
Nutrient use efficiency	**PPUE**	173.98 ± 4.06	128.16 ± 2.99	180.43 ± 5.01	144.98 ± 4.18	191.04 ± 4.55
	PNUE	7.54± 0.71	7.02±0.9	7.87±1.16	5.38 ± 1.09	8.14± 1.51
Metabolic traits	***P***	6.53 ± 0.30	12.86 ± 3.25	2.76 ± 0.45	7.37 ± 0.45	8.00 ± 1.72
	R	1.6 ± 0.14	3.88 ± 1.59	0.21 ± 0.06	2.10 ± 0.67	1.46 ± 0.76
	NP	1.70 ± 0.01	2.55 ± 0.56	1.17± 0.17	1.58 ± 0.15	2.54 ± 0.60
	Φ_{PSII}	0.41 ± 0.005	0.27 ± 0.006	0.29 ± 0.01	0.13 ± 0.04	0.24 + 0.02
	CUE	0.63 ± 0.12	0.71 ± 0.03	0.81 ± 0.10	0.67 ± 0.03	0.73 ± 0.01
Thermal	***E_a*** (eV)	0.36 ± 0.19	0.25 ± 0.08	0.57 ± 0.1	0.57 ± 0.09	0.91 ± 0.1

tolerance of growth	$\mu(T_c)$	-0.47 ± 0.11	-0.5 ± 0.11	-0.46 ± 0.15	-1.18 ± 0.16	-1.1 ± 0.16
	E_h(eV)	6.11 ± 2.95	4.8 ± 0.93	7.32 ± 1.29	2.86 ± 1.28	4.14 ± 1.29
	T_h **(K)**	305.46 ± 1.77		No treatment effect 308.16 ± 0.35		
	T_{opt} **(ºC)**	28.69 ± 0.61	30.89 ± 0.16	32.14 ± 0.29	31.08 ± 0.62	33.90 ± 0.92
Thermal response of *P*	E_a (eV)	1.07 ± 0.16		No treatment effect 0.87 ± 0.03		
	$P(T_c)$	-1.83 ± 0.12	-1.95± 0.15	-3.42 ± 0.11	-2.56 ± 0.13	-3.51 ± 0.11
	E_h(eV)	3.51 ± 0.29	3.24 ± 0.28	3.17 ± 0.39	2.98 ± 0.36	2.13 ± 0.36
	T_h (K)	303.41 ± 0.94	306.49 ± 0.55	306.49 ± 0.55	306.49 ± 0.55	306.49 ± 0.55
	T_{opt} (ºC)	27.27 ± 0.7	30.86 ± 0.02	32.03 ± 0.01	31.14 ± 0.04	33.37 ± 0.06
Thermal response of *R*	E_a (eV)	1.07 ± 0.16		No treatment effect 0.83 ± 0.04		
	$R(T_c)$	-2.54 ± 0.13	-2.57 ± 0.14	-3.92 ± 0.13	-2.74 ± 0.08	-3.84 ± 0.18
	E_h (eV)	2.54 ± 0.14	3.35 ± 0.46	2.66 ± 0.6	2.93 ± 0.52	1.74 ± 0.54
	T_h (K)	305.25 ± 0.94		No treatment effect 307.74 ± 0.81		
	T_{opt} (ºC)	28.82± 0.36	31.99 ± 0.01	32.62± 62	31.83 ± 0.42	33.95 ± 0.92

Table S2 | Model selection on generalised additive mixed effects model (GAMM) fitted to the trajectories of population growth. We fitted a GAMM to test whether the trajectories of population growth differed among the selection regimes. In the model, the effect of 'treatment' assesses whether median log-growth rates differ among selection regimes, while s(day.of.exp, by = selection regime) indicates whether the trajectories of growth rate differ among the selection regimes. Models were compared via the small sample-size corrected Akaike Information Criterion (AICc), delta AICc is the difference in AICc score relative to the model with the lowest value (most parsimonious model) and Weight is the relative support for the model. The best fitting models were selected as those returning the lowest AICc score and the highest AICc weight and are highlighted in bold.

Model selection table

formula = mue ~ treatment + s(day.of.exp, by = selection regime, bs='cr'), random = ~1 | selection regime/replicate

	Intercept	s(day.of.exp, treatment)	selection regime	df	logLik	AICc	Delta	Weight
4 (full model)	**0.71**	**+**	**+**	**15**	**276.1**	**-525.0**	**0**	**0.87**
2	0.73	+		12	271.99	-521.2	3.80	0.13
1	0.70			4	-50.26	399.0	923.93	0
3	0.66	+		7	-49.28	405.5	930.44	0

Table S3 | Model selection on generalised additive mixed effects model (GAMM) fitted to the trajectories of population size. We fitted a GAMM to test whether the trajectories of population size differed among the selection regimes. In the model, the effect of 'treatment' assesses whether median log-population size differ among selection regimes, while s(day.of.exp, by = treatment) indicates whether the trajectories of growth population size differ among the selection regimes. Models were compared via the small sample-size corrected Akaike Information Criterion (AICc)), delta AICc is the difference in AICc score relative to the model with the lowest value (most parsimonious model) and Weight is the relative support for the model. The best fitting models were selected as those returning the lowest AICc score and the highest AICc weight and are highlighted in bold.

Model selection table

formula = pop size~ treatment + s(day.of.exp, by = selection regime, bs='cr'), random = ~ 1 | selection regime/replicate

	Intercept	s(day.of.exp, treatment)	selection regime	df	Log Lik	AICc	Delta	Weight
4 (full model)	7.018	+	+	**11**	-489.3	9809.5	0	0.927
2	7.16	+		8	-489.9	9814.6	5.07	0.073
3	6.905			7	-493.8	9891.4	81.88	0
1	6.998	+		4	-494.3	9894.4	84.92	0

Table S4 | Thermal tolerance curve parameters for the ancestor. The thermal tolerance curve was quantified by fitting Eq. (6) to the growth rates quantified over a temperature gradient from 15ºC to 40ºC. CI (95%) are the lower and upper 95% confidence intervals.

Parameter	Environment	Estimate	CI (95%) [lower, upper]
$\mu(T_c)$	22	-0.47	[-1.12,-0.27]
E_a	22	0.35	[0.31,1.13]
E_h	22	6.12	[6.04,12.11]
T_h	22	305.46 K or 32.31ºC	[301.75,309.1] or ºC [28.62,36.01]

Table S5 | Model selection and parameters of thermal tolerance curves of the evolved lineages. The mechanistic temperature dependence function (see Eq. (6), also Fig. 1) was fitted to the growth rate quantified over a temperature gradient from 15ºC to 40ºC for all evolved lineages (see table S4 for analysis of the ancestor). Models included random effects on each of the parameters of Eq. (6) by replicate and 'selection environment' as a fixed four level factor on each parameter. Models were compared via the small sample-size corrected Akaike Information Criterion (AICc), delta AICc is the difference in AICc score relative to the model with the lowest value (most parsimonious model) and Weight is the relative support for the model. The best fitting models were selected as those returning the lowest AICc score and the highest AICc weight and are highlighted in bold. In the model output, CI (95%) are the lower and upper 95% confidence intervals.

Model selection table

Model name	Remove selection environment effect on	K	AICc	Delta	Weight	Log lik
resl.mix3	**T_h**	**18**	**218.81**	**0**	**0.78**	**-88.65**
resl.mix7	$E_h + T_h$	15	222.04	3.22	0.16	-94.13
resl.mix	NA - full model	21	223.81	4.99	0.06	-87.09
resl.mix11	$E_a + E_h + T_h$	12	239.43	20.62	0	-106.52
resl.mix6	Ea + T_h	15	239.93	21.11	0	-103.07
resl.mix4	$\mu(T_c)$	18	242.31	23.49	0	-100.39
resl.mix14	$\mu(T_c) + E_h + T_h$	12	243.14	24.32	0	-108.37
resl.mix12	$\mu(T_c) + E_a + E_h$	12	250.66	31.85	0	-112.13
resl.mix15	All	9	251.98	33.16	0	-116.31
resl.mix2	E_h	18	286.3	67.49	0	-122.39
resl.mix13	$\mu(T_c) + E_a + T_h$	12	299.85	81.04	0	-136.73
resl.mix10	$\mu(T_c) + T_h$	15	305.06	86.25	0	-135.64

resl.mix1	E_a - no convergence
resl.mix5	$E_a + E_h$ - no convergence

Model parameters

Parameter	Environment	Estimate	CI (95%) [lower, upper]
$\mu(T_c)$	22	-0.5	[-0.71,-0.29]
$\mu(T_c)$	26	-0.46	[-0.97,-0.01]
$\mu(T_c)$	32	-1.18	[-1.69,-0.66]
$\mu(T_c)$	FS	-1.1	[-1.62,-0.57]

E_a (eV)	22	0.25	[0.11,0.51]	
E_a(eV)	26	0.57	[0.21,0.91]	
E_a(eV)	32	0.57	[0.23, 0.91]	
E_a(eV)	FS	0.91	[0.57,1.25]	
E_h (eV)	22	4.8	[2.31,5.85]	
E_h (eV)	26	7.32	[3.28,12.13]	
E_h (eV)	32	2.86	[0.01,6.98]	
E_h (eV)	FS	4.14	[0.07,8.90]	
T_h	No treatment effect	308.16 K or 35.01ºC	[307.49,308.82]	or ºC [34.34, 35.67]

Table S6 | Model selection and parameters for the thermal responses of gross photosynthesis and respiration in the ancestor. Eq. (6) was fitted to the metabolic rates quantified over a temperature gradient from 7ºC to 40ºC (3ºC increments) for the ancestor using a non-linear mixed effects model. "Flux", i.e. respiration or photosynthesis, was fitted as a fixed two-level factor to test for differences in thermal responses for photosynthesis (P) and respiration (R), and model selection otherwise proceeded as described above. Models were compared via the small sample-size corrected Akaike Information Criterion (AICc), delta AICc is the difference in AICc score relative to the model with the lowest value (most parsimonious model) and Weight is the relative support for the model. The best fitting models were selected as those returning the lowest AICc score and the highest AICc weight and are highlighted in bold..

Model selection

Model name	Remove "flux" effect on	K	AICc	Delta	Weight	Log Lik
Mod4	E_a	8	217.19	0	0.976	-100.595
Mod2	$P(T_c)$	9	225.44	8.25	0.015	-103.72
Mod1	E_h	10	227.62	10.43	0.005	-103.81
Mod3	T_h	8	229.01	11.82	0.002	-106.505

Parameters

Parameter	Estimate	CI 95% [lower, upper]	
E_a (eV)	1.07	[0.73,1.44]	
$P(T_c)$	-1.83	[-2.98,-1.01]	
$R(T_c)$	-2.54	[-2.65,-1.59]	
E_h. P (eV)	3.51	[3.17,4.39]	
$E_h R$ (eV)	2.54	[2.35,3.53]	
T_h. P (K)	303.41 (K) or 30.26ºC	[301.29,305.9]	or ºC [28.14,32.8]
T_h.R (K)	305.25 or 32.10ºC	[294.88,306.9]	or ºC [21.73,33.84]

Table S7| Model selection and parameters for the thermal response of gross photosynthesis in the evolved lineages. Eq. (6) was fitted to the metabolic rates quantified over a temperature gradient from 7ºC to 40ºC (3ºC increments) for the evolved lineages using a non-linear mixed effects model. "Selection regime" was fitted as a fixed factor to test for differences in the parameters characterizing the thermal response for photosynthesis among the selection regimes. Models were compared via the small sample-size corrected Akaike Information Criterion (AICc), delta AICc is the difference in AICc score relative to the model with the lowest value (most parsimonious model) and Weight is the relative support for the model. The best fitting models were selected as those returning the lowest AICc score and the highest AICc weight and are highlighted in bold.

Model selection table

Model name	Remove selection regime effect on	K	AICc	Delta	Weight	Log Lik
gp.mix6	**E_a + T_h**	**14**	**300.28**	**0**	**0.46**	**-135.21**
gp.mix11	E_a + E_h + T_h	11	302.78	2.5	0.13	-139.81
gp.mix15	All	8	303.34	3.06	0.1	-143.36
gp.mix3	T_h	17	303.61	3.33	0.09	-133.43
gp.mix1	E_a	17	303.74	3.46	0.08	-133.5
gp.mix8	$P(T_c)$+ E_a	14	304.08	3.81	0.07	-137.11
gp.mix12	$P(T_c)$+ E_a+ E_h	11	305.4	5.12	0.04	-141.12
gp.mix7	E_h+ T_h	14	307.32	7.04	0.01	-138.73
gp.mix14	$P(T_c)$+E_h + T_h	11	307.72	7.44	0.01	-142.28
gp.mix	NA - full model	20	309.34	9.06	0	-132.76
gp.mix4	$P(T_c)$	17	309.64	9.36	0	-136.45
gp.mix2	E_h	17	310.05	9.78	0	-136.65
gp.mix13	$P(T_c)$+E_a+T_h	11	312.68	12.41	0	-144.77
gp.mix5	E_a + E_h - no converfence					
gp.mix9	$P(T_c)$+ E_h - no convergence					

Parameters

Treatment effect on	Environment	Estimate	CI (95%)
$P(T_c)$	22	-1.95	[-2.01,-1.12]
$P(T_c)$	26	-3.92	[-4.09,-2.28]
$P(T_c)$	32	-2.47	[-3.03,-1.92]
$P(T_c)$	FS	-3.84	[-4.44,-2.42]
E_a (eV)	No treatment effect	0.87	[0.81,0.94]

E_h (eV)	22	3.24	[2.71, 3.82]	
E_h (eV)	26	3.17	[1.95, 4.55]	
E_h (eV)	32	2.98	[1.74,4.23]	
E_h(eV)	FS	2.13	[0.89, 3.41]	
T_h	No treatment effect	306.49 K (or 33.34ºC)	[303.42, 307.57]	Or ºC [30.27,34.42]

Table S8 | Model selection and parameters for the thermal response of respiration in the evolved lineages. Eq. (6) was fitted to the metabolic rates quantified over a temperature gradient from 7ºC to 40ºC (3ºC increments) for the evolved lineages using a non-linear mixed effects model. "Selection regime" was fitted as a fixed factor to test for differences in the parameters characterizing the thermal response for respiration among the selection regimes. Models were compared via the small sample-size corrected Akaike Information Criterion (AICc), delta AICc is the difference in AICc score relative to the model with the lowest value (most parsimonious model) and Weight is the relative support for the model. The best fitting models were selected as those returning the lowest AICc score and the highest AICc weight and are highlighted in bold.

Model selection table

Model name	Remove selection environment effect on	K	AICc	Delta	Weight	Log Lik
r.mix6	**E_a + T_h**	**15**	**279.94**	**0**	**0.64**	**-123.83**
r.mix11	**E_a + E_h + T_h**	**12**	**281.84**	**1.9**	**0.25**	**-128.19**
r.mix1	E_a	18	284.95	5.01	0.05	-122.82
r.mix3	T_h	18	285.45	5.51	0.04	-123.07
r.mix7	E_h + T_h	15	288.51	8.57	0.01	-128.11
r.mix15	All	9	290.74	10.81	0	-135.96
r.mix	NA- full model	21	291.51	11.57	0	-122.49
r.mix8	$R(T_c)$+E_a	15	293.18	13.24	0	-130.45
r.mix12	$R(T_c)$+ E_a + E_h	12	293.77	13.83	0	-134.15
r.mix9	$R(T_c)$+ E_h	15	295.98	16.05	0	-131.85
r.mix14	$R(T_c)$+ E_h + T_h	12	297.2	17.26	0	-135.87
r.mix4	$R(T_c)$	18	299.26	19.32	0	-129.98
r.mix2	E_h	18	299.37	19.43	0	-130.03
r.mix10	$R(T_c)$+T_h	15	303.08	23.14	0	-135.4
r.mix13	$R(T_c)$+ E_a + T_h	12	306.02	26.08	0	-140.28
r.mix5	E_a + E_h - no convergence					

Evolved samples - components of the two best models

	df	logLik	AICc	Delta	weight
r.mix6	15	-123.83	279.94	0	0.72
r.mix11	12	-128.19	281.84	1.9	0.28

Parameter estimates for Delta AICc <2				
$R(T_c)$	E_a (eV)	E_h (eV)	T_h K	T_h ºC

22 ºC	-2.57	0.83 (no treatment effect)	3.35	307.47 (no treatment effect)	34.59 (no treatment effect)
26ºC	-3.92		2.66		
32ºC	-2.74		2.93		
FS	-3.84		1.74		

Sum of AIC based relative weights

	$R(T_c)$	E_a (eV)	E_h (eV)	T_h	
	0.99	0.05	0.73	0.05	

95% interval

	$R(T_c)$	E_a (eV)	E_h (eV)	T_h K	T_h ºC
22 ºC	[-2.62, -1.38]	[0.71,0.84]	[2.43,4.26]	[305.82,310.5]	[32.67,37.48]
26ºC	[-4.01, -2.09]	(no treatment effect)	[0.54,4.78]	(no treatment effect)	
32ºC	[-3.51, -1.54]		[0.96,4.87]		
FS	[-3.80, -1.82]		[0.26,3.74]		

Table S9 | Model selection to determine the effects of selection regime on the carbon use efficiency. We fitted the CUE data to a linear mixed model to test whether CUE differed among the selection regimes. Models were compared via the small sample-size corrected Akaike Information Criterion (AICc), delta AICc is the difference in AICc score relative to the model with the lowest value (most parsimonious model) and Weight is the relative support for the model. The best fitting models were selected as those returning the lowest AICc score and the highest AICc weight and are highlighted in bold. The best fitting model included differences in CUE among the selection regimes.

Model selection table							
Formula	fixed = cue ~ selection regime, random = ~1 | selection regime/replicate						
Model	**Intercept**	**selection regime**	**Df**	**logLik**	**AICc**	**Delta**	**weight**
2	**0.63**	**+**	**7**	**35.84**	**-53.70**	**0.00**	**1.00**
1	0.68		3	22.37	-38.00	15.69	0.00

Parameter estimates and 95% Confidence intervals		
Selection regime	**Parameter Estimate**	**95% Confidence interval [lower, upper]**
Ancestor	0.63	[0.59, 0.67]
22ºC	0.71	[0.65, 0.77]
26ºC	0.81	[0.77, 0.85]
32ºC	0.67	[0.61, 0.73]
FS	0.71	[0.69, 0.73]

Table S10| Model selection for the light response curves of photochemical efficiency. An exponential decay function (see Eq. (8)) was fitted to the photochemical efficiency (ϕ_{PSII}) light response curves using a non-linear mixed effects model. "Selection regime" was fitted as a fixed factor to test for differences in the parameters characterizing the light response curves for between the ancestor and the selection regimes. Models were compared via the small sample-size corrected Akaike Information Criterion (AICc), delta AICc is the difference in AICc score relative to the model with the lowest value (most parsimonious model) and Weight is the relative support for the model. The best fitting models were selected as those returning the lowest AICc score and the highest AICc weight and are highlighted in bold.

Model selection for ϕ_{PSII} ancestor populations

Model	Df	Assay temperature effect dropped on	AICc	Log Lik	Delta	Weight
Full	**9**		**-1087.66**	**552.83**	**0**	**0.74**
Exp.mix2	7	Slope b	-956.38	485.19	131.28	0.24
Exp.mix1	7	Intercept a	-695.53	354.76	392.21	0.02

Model selection for ϕ_{PSII} evolved populations

Model	Df	Selection regime effect dropped on	AICc	LogLik	Delta	Weight
Full	**11**		**-1554.52**	**-1512.54**	**0**	**0.84**
Exp.mix1	8	Intercept a	-1540.76	-1510.21	13.76	0.09
Exp.mix2	8	Slope b	-1540.39	-1509.85	14.13	0.07

Parameter estimates and 95% confidence intervals

Selection regime and parameter	**Estimate**	**95% confidence interval [lower, upper]**
Slope Ancestor (at 22ºC)	- 0.0013	[-0.0014, -0.0012]
Intercept Ancestor (at 22º)	0.51	[0.49, 0.53]
Slope Ancestor (at 26ºC)	- 0.0009	[-0.001, -0.0008]
Intercept Ancestor (at 26ºC)	0.31	[0.29, 0.32]
Slope Ancestor (at 32ºC)	- 0.0029	[-0.005, -0.0009]
Intercept Ancestor (at 32ºC)	0.21	[0.19, 0.23]
Slope evolved 22ºC	-0.0012	[-0.0014, -0.0010]
Intercept evolved 22ºC	0.36	[0.32, 0.40]
Slope evolved 26ºC	-0.0009	[-0.0011, -0.0007]
Intercept evolved 26ºC	0.41	[0.39, 0.43]

Slope evolved 32ºC	-0.0005	[-0.0006, -0.0004]
Intercept evolved 32ºC	0.56	[0.54, 0.58]
Slope evolved FS	-0.0008	[-0.0007, -0.0009]
Intercept evolved FS	0.46	[0.44, 0.48]

Table S11| Model selection for C:N, C:P, N:P, PPUE, PNUE, Chl:C ratio, size and silicate content, as well as Φ_{PSII} at irradiance as in the incubator. All traits were analyzed using separate mixed effects models, where 'selection regime' was a fixed effect and replicate nested within selection regime was a random effect on the intercept. In all traits, there was a significant effect of selection regime. Models were compared via the small sample-size corrected Akaike Information Criterion (AICc), delta AICc is the difference in AICc score relative to the model with the lowest value (most parsimonious model) and Weight is the relative support for the model. The best fitting models were selected as those returning the lowest AICc score and the highest AICc weight and are highlighted in bold.

Model selections

C:N

Global Model: fixed = CN ~ selection regime, random = ~1 | selection regime/replicate

Model	Intercept	selection regime	Df	logLik	AICc	delta	weight
2	**7.07**	**+**	**7**	**-76.05**	**167.50**	**0**	**0.99**
1	7.18		3	-88.973	183.60	16.07	0.01

N:P

Global Model: fixed = NP ~ selection regime, random = ~1 | selection regime/replicate

Model	Intercept	selection regime	Df	logLik	AICc	delta	weight
2	**10.16**	**+**	**7**	**-195.04**	**405.40**	**0**	**1.00**
1	12.46		3	-209.91	426.1	20.66	0

C:P

Global Model: fixed = CP ~ selection regime, random = ~1 | selection regime/replicate

Model	Intercept	selection regime	Df	logLik	AICc	Delta	weight
2	**70.77**	**+**	**7**	**-393.15**	**801.70**	**0.00**	**1.00**
1	90.72		3	-406.84	820	18.27	0.00

Silicate

Global Model: fixed = Si ~ selection regime, random = ~1 | selection regime/replicate

Model	Intercept	selection regime	Df	logLik	AICc	delta	weight
2	**0.35**	**+**	**7**	**-72.67**	**160.7**	**0**	**0.83**
1	0.39		3	-78.78	163.8	3.14	0.17

PPUE

Global Model: fixed =PPUE ~ selection regime, random = ~1 | selection regime/replicate

Model	Intercept	selection	Df	logLik	AICc	delta	weight

		regime					
2	**173.98**	**+**	**7**	**-268.46**	**513.8**	**0**	**0.95**
1	190.8		3	-273.82	554.2	40.4	0.05

PNUE

Global Model: fixed = PNUE ~ selection regime, random = ~1 | selection regime/replicate

Model	Intercept	selection regime	Df	logLik	AICc	delta	weight
2	**7.54**	**+**	**7**	**-121.72**	**260.3**	**0**	**0.87**
1	8.75		3	-128.74	264	3.73	0.13

Cell volume

Global Model: fixed = Size ~ selection regime, random = ~1 | selection regime/replicate

Model	Intercept	selection regime	Df	logLik	AICc	delta	weight
2	**3794**	**+**	**7**	**-2032.12**	**4078.8**	**0**	**1**
1	5776		3	-2048.43	4103	24.17	0

Chlorophyll:C ratio

Global Model: fixed = Chl:C ~ selection regime, random = ~1 | selection regime/replicate

Model	Intercept	selection regime	Df	logLik	AICc	delta	weight
2	**0.02**	**+**	**7**	**413.58**	**-812.6**	**0**	**1**
1	0.08		3	352.88	-699.6	112.95	0

Φ_{PSII}

Global Model: fixed = Φ_{PSII} ~ selection regime, random = ~1 | selection regime/replicate

Model	Intercept	selection regime	Df	logLik	AICc	delta	weight
2	**0.12**	**+**	**6**	**137.86**	**-263.71**	**0**	**0.81**
1	0.15		3	124.28	-242.56	21.15	0.19

Parameter estimates and 95% confidence intervals

C:N

Selection regime	**Parameter estimate**	**95% Confidence interval [lower, upper]**
Ancestor	7.07	[7.02, 7.12]
22ºC	6.94	[6.82, 7.06]
26ºC	7.08	[7.07, 7.09]

32ºC	7.21	[7.08, 7.34]
FS	7.18	[7.09, 7.27]

N:P

Selection regime	Parameter estimate	95% Confidence interval [lower, upper]
Ancestor	10.16	[9.93, 10.39]
22ºC	10.14	[9.85, 10.43]
26ºC	12.75	[12.44, 13.06]
32ºC	15.07	[14.81, 15.33]
FS	13.21	[12.76, 13.66]

C:P

Selection regime	Parameter estimate	95% Confidence interval [lower, upper]
Ancestor	70.78	[67.91, 73.65]
22ºC	69.91	[67.16, 72.66]
26ºC	84.91	[82.25, 87.57]
32ºC	112.93	[109.22, 116.64]
FS	93.22	[84.32, 102.12]
FS	0.202	[0.186, 0.218]

Picomol Si per cell

Selection regime	Parameter estimate	95% Confidence interval [lower, upper]
Ancestor	0.353	[0.347, 359]
22ºC	0.317	[0.314, 0.320]
26ºC	0.346	[0.336, 0.356]
32ºC	0.168	[0.158, 0.178]
FS	0.311	[0.309, 0.313]

PPUE

Selection regime	Parameter estimate	95% Confidence interval [lower, upper]
Ancestor	17.98	[13.92, 22.04]
22ºC	128.16	[125.17, 131.15]
26ºC	180.43	[175,42. 185, 44]
32ºC	144.98	[140.8, 149.16]
FS	191.04	[168.49, 195.59]

PNUE

Selection regime	Parameter estimate	95% Confidence interval [lower, upper]
Ancestor	7.54	[7.06, 7.82]
22ºC	7.02	[6.65, 7.38]
26ºC	7.87	[7.4, 8.34]

32ºC	5.38	[4.9, 5.78]
FS	8.14	[7.52, 8.76]

Cell volume

Selection regime	Parameter estimate	95% Confidence interval [lower, upper]
Ancestor	3794.25	[3113.64, 4474.86]
22ºC	3610.65	[2821.51, 4399.79]
26ºC	6359.75	[5541.58, 7177.92]
32ºC	8588.82	[7895.87, 9281.77]
FS	4643.54	[3969.93, 5317.15]

Chlorophyll:C ratio

Selection regime	Parameter estimate	95% Confidence interval [lower, upper]
Ancestor	0.024	[0.017, 0.031]
22ºC	0.071	[0.069, 0.073]
26ºC	0.121	[0.119, 0.123]
32ºC	0.088	[0.082, 0.094]
FS	0.085	[0.078, 0.092]

Φ_{PSII} at Iopt

Selection regime	Parameter estimate	95% Confidence interval [lower, upper]
Ancestor	0.12	[0.119, 0.121]
22ºC	0.09	[0.082, 0.098]
26ºC	0.12	[0.112, 0.128]
32ºC	0.08	[0.073, 0.087]
FS	0.12	[0.119, 0.121]

Table S12| PERMANOVA and pairwise comparisons based on treatment-level divergence in single nucleotide polymorphisms. Using only non-synonymous single nucleotide polymorphisms (SNPs), we quantified the number of sites that acquired mutations in each population relative to the ancestral reference sequence, and from allele frequencies, the genetic distance of each population from the ancestor and the genetic divergence among populations. A distance matrix was then calculated from Euclidean distances and passed to permutational multivariate analysis of variance (PERMANOVA) to assess overall treatment effects and individual pairwise differences between levels of the treatment were assessed with TukeyHSD tests.

ANOVA Table	**SNPs**					
Response:	Distances					
	Df	Sum Sq	Mean Sq	F value	Pr(>F)	
Treatment	4	0.31587	0.078967	5.1919	0.007097	**
Residuals	16	0.24335	0.01521			

Pairwise distances				
Comparison	Difference	Lower 95% CI	Upper 95% CI	P
26-22	0.129	0.015	0.373	0.045
32-22	0.023	0.005	0.242	0.047
32-26	-0.106	-0.350	0.138	0.677
Anc-22	-0.469	-0.877	-0.061	0.021
Anc-26	-0.598	-1.020	-0.176	0.004
Anc-32	-0.492	-0.900	-0.084	0.015
FS-22	0.104	0.040	0.348	0.039
FS-26	-0.025	-0.292	0.002	0.050
FS-32	0.081	0.003	0.325	0.050
FS-Anc	0.573	0.151	0.995	0.006

Table S13| PERMANOVA and pairwise comparisons based on treatment-level divergence in phenotypic traits. Phenotypic trait values of a population in its selection environment after 300 generations of evolution were normalised relative to the trait values of the ancestor in that same environment. The traits investigated were gross photosynthesis at saturating light intensity and incubator light intensity, growth and respiration rates, intracellular stoichiometry (ratios and amounts per cell), cell size, chlorophyll content, FRRF data (dark adapted F_v/F_m at incubator and saturating light intensity, and as a function of light intensity for photosynthetic efficiency, relative rate of electron transport through PSII, *C* as the proportion of PSII reaction centres in a closed state, and NPQ as non-photochemical quenching), and flow cytometry data (side scatter for granularity, FL1 fluorescence after a rhodamine dye as a proxy for H+ transport across mitochondrial membranes, FL2 and FL3 fluorescence after a Nile Red dye as a proxy for intracellular lipid content).The phenotypic trait data were then analysed through calculating a difference matrix and using permutational multivariate analysis of variance (PERMANOVA) to assess overall treatment effects and individual pairwise differences between levels of the treatment were assessed with TukeyHSD tests.

ANOVA Table	**Phenotype**					
Response:	Distances					
	Df	Sum Sq	Mean Sq	F value	Pr(>F)	
Treatment	4	3.3427	0.83568	3.3174	0.03075	*
Residuals	20	5.0382	0.25191			

Pairwise distances				
Comparison	Difference	Lower 95% CI	Upper 95% CI	P
26-22	0.69	0.17	1.56	0.051
32-22	0.38	0.19	1.25	0.049
Anc-22	-1.04	-2.66	-0.28	0.034
FS-22	0.39	0.18	1.25	0.047
32-26	-0.31	-1.18	-0.15	0.048
Anc-26	-1.73	-3.35	-0.11	0.033
FS-26	-0.31	-1.17	0.56	0.827
Anc-32	-1.42	-3.04	-0.20	0.010
FS-32	0.01	-0.86	0.88	0.100
FS-Anc	1.43	0.82	3.05	0.020

Table S14| Table of genes where SNPs were the most strongly associated with treatment. The top 20 loadings were pulled from a SNP based PCA where treatments had been found to cluster differently. aGene denotes the gene name (accessible through NCBI), "from component" denotes whether the gene was pulled from the first (comp1) or second (comp2) principal component. Associated with treatment denotes the selection regime that the gene was the most strongly associated with. Function gives an overview of the function if known and 'other', additional information on the gene and its putative functions. Gene functions were sourced from UniProt and NCBI.

Gene accession code	From component	Associacted with treatment	Function	Additional information
THAPSDRAFT_23994	comp1	FS	Thiol-dependent ubiquitinyl hydrolase activity	uncharacterised, function inferred from homology
RPT5.1	comp2	32	26S proteosome ATPase regulatory subunit	Positive regulation of RNA polymerase II transcriptional preinitiation complex assembly
THAPSDRAFT_5389.1	comp2	26	Alpha-1,3-glucosyltransferase,This protein is involved in the pathway protein glycosylation, which is part of Protein modification.	function inferred from homology
THAPSDRAFT_5001.1	comp2	FS	ATP binding	uncharacterised, function inferred from homology
THAPSDRAFT_bd1378	comp1	26	ATP synthase subunit a, chloroplastic	function inferred from homology
THAPSDRAFT_11712	comp1	26	uncharacterised transmembrane protein	unknown
THAPSDRAFT_bd1563	comp1	32	ATP synthase subunit beta	Produces ATP from ADP in the presence of a proton gradient across the membrane.
THAPSDRAFT_bd1318	comp1	32	ATP synthase subunits	Produces ATP from ADP in the presence of a proton gradient across the membrane.
THAPSDRAFT_264016	comp1	26	Calcium transporting rt-atpase	ATP binding function has been inferred from homology
THAPSDRAFT_21124	comp1	26	unknown	unknown
THAPSDRAFT_bd1611	comp1	22	Chlorophyll binding	function inferred from homology
THAPSDRAFT_bd1439	comp1	32	Chloroplast component	uncharacterised, function inferred from homology
THAPSDRAFT_11407	comp1	26	unknown	unknown
THAPSDRAFT_bd2063	comp1	FS	Chloroplast component	uncharacterised, function inferred from homology
THAPSDRAFT_bd1441	comp1	32	Cytochrome c biogenesis protein	Required during biogenesis of c-type cytochromes

			CcsA	(cytochrome c6 and cytochrome f) at the step of heme attachment, inferred from homologies
THAPSDRAFT_4075	comp2	32	DNA binding	uncharacterised, function inferred from homology
THAPSDRAFT_bd997	comp1	32	DNA-dependent RNA polymerase	catalyses the transcription of DNA into RNA using the four ribonucleoside triphosphates as substrates
THAPSDRAFT_21370	comp1	26	unknown	unknown
THAPSDRAFT_bd1267	comp1	26	DNA-dependent RNA polymerase catalyses the transcription of DNA into RNA using the four ribonucleoside triphosphates as substrates	Inferred from homologues
THAPSDRAFT_bd2050	comp1	32	DNA-dependent RNA polymerase, second subunit	catalyzes the transcription of DNA into RNA using the four ribonucleoside triphosphates as substrates
THAPSDRAFT_2462.1	comp2	26	unknown	unknown
THAPSDRAFT_4767.1	comp2	26	unknown	unknown
THAPSDRAFT_bd846.1	comp2	26	unknown	unknown
THAPSDRAFT_8190.1	comp2	26	unknown	unknown
THAPSDRAFT_bd1736	comp1	26	Electron transporter, transferring electrons within the cyclic electron transport pathway of photosynthesis activity	function inferred from homology
THAPSDRAFT_22706	comp1	26	Endonuclease	function inferred from homology
THAPSDRAFT_bd1258	comp1	FS	Ferredoxin	Iron-sulphur proteins that transfer electrons in a wide variety of metabolic reactions, e.g. electron chain in photosynthesis
THAPS_25392	comp1	26	Hypothetical integral component of membrane	details unknown
THAPSDRAFT_2049	comp1	26	Hyrdrolase acticity	function inferred from homology
THAPSDRAFT_4495.1	comp2	32	Integral membrane component	uncharacterised, function inferred from homology
THAPSDRAFT_37979.1	comp2	32	Iron-sulphur cluster assembly	uncharacterised, function inferred from homology
THAPSDRAFT_867	comp1	32	unknown	unknown
THAPSDRAFT_2407	comp1	32	unknown	unknown

THAPSDRAFT_bd1360	comp1	22	Iron-sulphur cluster formation ABC transporter, plastid protein	function inferred from homology
THAPSDRAFT_7957.1	comp2	32	unknown	unknown
THAPSDRAFT_4573.1	comp2	32	unknown	unknown
THAPSDRAFT_7448.1	comp2	32	unknown	unknown
THAPSDRAFT_7815.1	comp2	32	unknown	unknown
THAPSDRAFT_34293.1	comp2	32	Metal ion binding, pre-mRNA binding	uncharacterised, function inferred from homology
THAPSDRAFT_7696.1	comp2	32	unknown	unknown
THAPSDRAFT_9243.1	comp2	32	unknown	unknown
THAPS_6723.1	comp2	32	unknown	unknown
THAPSDRAFT_bd980	comp1	FS	Mg-protoporphyrin IX chelatase	Involved in chlorophyll biosynthesis. Catalyzes the insertion of magnesium ion into protoporphyrin IX to yield Mg-protoporphyrin IX
THAPSDRAFT_23775.1	comp2	32	unknown	unknown
THAPSDRAFT_3141.1	comp2	32	unknown	unknown
THAPSDRAFT_9591.1	comp2	32	unknown	unknown
THAPSDRAFT_2441.1	comp2	32	unknown	unknown
THAPSDRAFT_264303.1	comp2	32	unknown	unknown
THAPS_263324	comp2	32	unknown	unknown
THAPSDRAFT_bd705	comp2	32	unknown	unknown
THAPSDRAFT_2244.1	comp2	32	unknown	unknown
THAPSDRAFT_8234	comp1	FS	Nucleic acid binding	uncharacterised, function inferred from homology
THAPSDRAFT_11408	comp1	FS	Nucleic acid binding	uncharacterised, function inferred from homology
THAPSDRAFT_8715.1	comp2	32	unknown	unknown
THAPSDRAFT_33926.1	comp2	32	Obtusifoliol 14-alpha demethylase	iron-binding, also CH3 transferase, function inferred from homology
THAPSDRAFT_bd1013	comp1	26	Peroxidase	function inferred from homology
THAPSDRAFT_264058.	comp2	32	Phosphatase 2A (PP2A) regulatory	calcium ion binding, function inferred from homology

1			subunit B-like protein-like protein	
THAPS_6819.1	comp2	32	Phospholipid biosynthetic process	uncharacterised, function inferred from homology
THAPSDRAFT_943	comp2	32	unknown	unknown
THAPSDRAFT_bd1545	comp1	26	Photosystem II CP43 reaction center protein	One of the components of the core complex of photosystem II (PSII). It binds chlorophyll and helps catalyze the primary light-induced photochemical processes of PSII.
THAPSDRAFT_bd1327	comp1	32	Replicative DNA helicase	DNA replication. In the process, it makes ADP and phosphate from ATP and H2O. ATP binding properties
THAPSDRAFT_bd1911	comp1	22	Ribosomal protein	RNA binding, known function
THAPSDRAFT_bd1447	comp1	26	Ribosomal protein, RNA binding	function inferred from homology
THAPSDRAFT_bd2088	comp1	FS	Ribulose bisphosphate carboxylase large chain	
THAPS_6735.1	comp2	32	unknown	unknown
THAPSDRAFT_6456.1	comp2	32	unknown	unknown
THAPSDRAFT_6600.1	comp2	32	RNA binding	uncharacterised, function inferred from homology
THAPS_35239	comp1	26	RNA binding, mRNA splicing	function inferred from homology
THAPS_6656.1	comp2	32	RNA binding, mRNA splicing	uncharacterised, function inferred from homology
THAPSDRAFT_31035.1	comp2	22	Serine-type endopeptidase activity	uncharacterised, function inferred from homology
THAPSDRAFT_19465.1	comp2	32	Thioredoxin-disulfide reductase activity	Catalyses NADP to NADPH reactions, function inferred from homology
THAPSDRAFT_268574	comp2	32	Tim22-like protein, protein channel	Protein localisation to organelle, function inferred from homology
THAPSDRAFT_24862	comp1	FS	unknown	unknown
THAPSDRAFT_6004	comp1	FS	unknown	unknown
THAPSDRAFT_267946	comp2	32	transferase activity	uncharacterised, function inferred from homology
THAPSDRAFT_24873	comp1	FS	unknown	unknown
THAPSDRAFT_7790	comp1	26	Transmembrane protein	details unknown
THAPSDRAFT_bd93	comp1	FS	Transmembrane protein	uncharacterised, function inferred from homology
THAPSDRAFT_10699	comp1	FS	unknown	unknown

THAPSDRAFT_17859.1	comp2	32	Transmembrane protein in endoplasmatic reticulum	uncharacterised, function inferred from homology

Table 15: Aligned sequence depths for each sequenced population. After trimming and filtering, remaining sequence reads were then aligned against version 2 of the reference *T. pseudonana* genome sequence (GenBank: GCA_000149405.2) using BWA-mem version 0.7.5a-2 with default settings . This resulted in average aligned sequence depths from 3.4 to 74.5 X; the average alignment depth for the t0 (ancestor) sample was 18.5 X. This resulted in a set of 64 BAM-formatted files. Depths and insert lengths were calculated using Qualimap.

Population name	Mean aligned sequence depth (X)	Accession number	Mapping quality mean	Median insert length (b.p.)
t0_S45	18.46	**To be added once granted by NCBI**	57.47	317.0
t300_22_b1_S19	18.39		57.54	281.0
t300_22_b2_S20	18.61		57.48	339.0
t300_22_b3_S21	17.66		57.6	259.0
t300_22_b4_S22	17.57		57.61	229.0
t300_22_b5_S23	18.52		57.45	333.0
t300_22_b6_S24	18.29		57.58	274.0
t300_26_b1_S25	18.65		52.83	345.0
t300_26_b2_S26	6.67		57.63	170.0
t300_26_b3_S27	15.02		57.72	109.0
t300_26_b4_S28	15.25		57.59	120.0
t300_26_b5_S29	18.71		57.48	353.0
t300_26_b6_S14	18.61		57.38	439.0
t300_32_b1_S3	18.65		57.53	431.0
t300_32_b2_S4	18.75		57.35	502.0
t300_32_b3_S5	18.68		57.45	489.0
t300_32_b4_S10	18.58		57.38	441.0
t300_32_b5_S9	18.41		57.4	391.0
t300_32_b6_S8	18.28		57.35	348.0
t300_FL_b1_S37	6.45		57.32	55.0
t300_FL_b2_S18	18.62		57.41	418.0
t300_FL_b3_S19	18.49		57.42	365.0
t300_FL_b4_S20	18.64		57.46	334.0
t300_FL_b5_S21	18.59		57.38	400.0
t300_FL_b6_S22	18.63		57.37	409.0
t300_FS_b1_S31	8.71		57.51	276.0
t300_FS_b2_S7	18.62		57.39	426.0
t300_FS_b3_S33	7.11		57.42	307.0
t300_FS_b4_S6	18.74		57.36	509.0

t300_FS_b5_S35	15.83	57.45	319.0
t300_FS_b6_S36	18.62	57.5	290.0